applied sciences

MDPI

Article

Identification of Transcription Factors, Biological Pathways, and Diseases as Mediated by N6-methyladenosine Using Tensor Decomposition-Based Unsupervised Feature Extraction

Y-h. Taguchi [1,*], S. Akila Parvathy Dharshini [2] and M. Michael Gromiha [2]

[1] Department of Physics, Chuo University, Tokyo 112-8551, Japan
[2] Department of Biotechnology, Bhupat and Jyoti Mehta School of Biosciences, Indian Institute of Technology Madras, Chennai 600036, Tamilnadu, India; akilabioinfo@gmail.com (S.A.P.D.); gromiha@iitm.ac.in (M.M.G.)
* Correspondence: tag@granular.com

Abstract: N^6-methyladenosine (m6A) editing is the most common RNA modification known to contribute to various biological processes. Nevertheless, the mechanism by which m6A regulates transcription is unclear. Recently, it was proposed that m6A controls transcription through histone modification, although no comprehensive analysis using this dataset was performed. In this study, we applied tensor decomposition (TD)-based unsupervised feature extraction (FE) to a dataset composed of mouse embryonic stem cells (mESC) and a human cancer cell line (HEC-1-A) and successfully identified two sets of genes significantly overlapping between humans and mice (63 significantly overlapped genes among a total of 16,763 genes common to the two species). These significantly overlapped genes occupy at most 10% genes from both gene sets. Using these two sets of genes, we identified transcription factors (TFs) that m6A might recruit, biological processes that m6A might contribute to, and diseases that m6A might cause; they also largely overlap with each other. Since they were commonly identified using two independent datasets, the results regarding these TFs, biological processes, and diseases should be highly robust and trustworthy. It will help us to understand the mechanisms by which m6A contributes to biological processes.

Keywords: N^6-methyladenosine; histone modification; tensor decomposition; feature extraction

Citation: Taguchi, Y.-h.; Dharshini, S.A.P.; Gromiha, M.M. Identification of Transcription Factors, Biological Pathways, and Diseases as Mediated by N6-methyladenosine Using Tensor Decomposition-Based Unsupervised Feature Extraction. *Appl. Sci.* **2021**, *11*, 213. https://dx.doi.org/10.3390/app11010213

Received: 28 October 2020
Accepted: 23 December 2020
Published: 28 December 2020

1. Introduction

Epitranscriptomics [1] generally attracts broad interest. It involves the post-transcriptional editing of RNA. Since this has not been comprehensively investigated, epitranscriptomics is hardly understood, in spite of its ubiquitous nature. A-to-I RNA editing [2] replaces adenosine with inosine, which is usually regarded as guanine. Thus, A-to-I RNA editing can alter the amino acid sequence of a protein translated from A-to-T edited RNA. Similarly, C-to-U [3] editing replaces cytosine with uracil, which also might result in alterations in amino acid sequences. Although the effects of A-to-I and C-to-U are relatively easy to understand, the other effects of epitranscriptomics are not always easy to understand. Such editing is mediated by various components, including Mettl3 [4] and Mettl14 [5]—used in the most frequently observed form of RNA editing in transcripts that are believed to affect a wide range of biological processes, ranging from development [6] to diseases [7]. It has been reported to be related to Alzheimer's disease [8] and Parkinson's disease [9]. It is also associated with various cancers [10] and plays several roles in immunity [11].

N^6-methyladenosine also has a relationship with epigenetics. Histone H3 trimethylation at lysine 36 guides m6A RNA modification co-transcriptionally [12]. The m6A of chromosome-associated regulatory RNA regulates chromatin state and transcription [13]. m6A modification controls circular RNA immunity [14].

In spite of these findings, the mechanism by which m6A affects gene expression profiles is unclear. Although there are many studies, most of them remain association

studies. For example, Akhtar et al. found that m6A increases RNAP II pause, in contrast they did not identify a detailed mechanism, and the studies remained simply identifications of links between RNAP II pausing and the m6A RNA modification [15]. Liu et al. found that m6A on chromosome-associated regulatory RNAs can globally tune chromatin state and transcription; nevertheless, this again remained an association study [13]. Zhou et al. found that m6A regulates alternative splicing [16]. Yang et al. found that m6A promotes R-loop formation [17]. In spite of only a few examples of studies on the mechanism that m6A regulates transcription, most of them remained as association studies. In this sense, it is important to find some elements that can affect transcription associated with m6A, even if it is a simple association study. Liu et al. [13] recently found that m6A can regulate transcription through histone modification; however, they did not specify the genes whose expressions were potentially affected by m6A. Histone modification is the addition of small molecules, e.g., methylation and acetylation, to histone tails that control chromatin structures. In this study, we applied tensor decomposition (TD)-based unsupervised feature extraction (FE) [18] in order to identify potential target genes whose expression is affected by m6A through histone modifications. As a result, we identified transcription factors that might be recruited by m6A, biological processes that might include genes whose expression is affected by m6A, and diseases caused by gene expression altered by m6A between mice and humans.

2. Materials and Methods

Figure 1 shows the flowchart of analyses performed in this study.

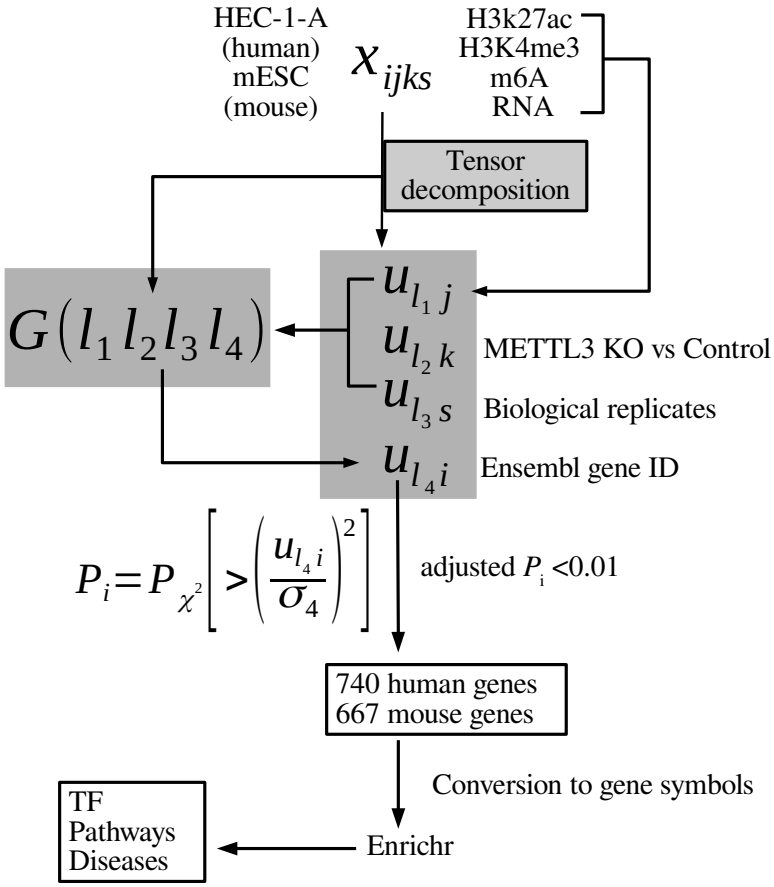

Figure 1. The flowchart of analyses performed in this study.

2.1. m6A, Histone Modification, and Gene Expression

m6A, histone modification, and gene expression data of a human cancer cell line (HEC-1-A) and mouse embryonic stem cells (mESC) were downloaded from Gene Expression Omunibus (GEO) [19] with GEO ID GSE140561 and GSE133600, respectively. The former dataset comprises H3K4me3, H3K27ac, MeRIP, and nascent nuclear RNA expressions of control or METTL3 KO cell lines, with two biological replicates (in total, 16 samples; Table 1), while the latter is composed of data from wild-types or either of two METTL3 KO mESC, with two biological replicates (in total, 24 samples; Table 2). For both sets, files whose names ended by ".gz" were retrieved from the "Supplementary file" section available from GEO.

Table 1. Sample tables for HEC-1-A human cancer cell lines.

GEO ID	Treatments	Observed	Replicates
GSM4174073	Control	H3K4me3	r1
GSM4174074	Control	H3K4me3	r2
GSM4174075	KD	H3K4me3	r1
GSM4174076	KD	H3K4me3	r2
GSM4174077	Control	H3K27ac	r1
GSM4174078	Control	H3K27ac	r2
GSM4174079	KD	H3K27ac	r1
GSM4174080	KD	H3K27ac	r2
GSM4174099	Control	MeRIP	r1
GSM4174100	Control	MeRIP	r2
GSM4174101	KD	MeRIP	r1
GSM4174102	KD	MeRIP	r2
GSM4174167	Control	nuclearRNA	r1
GSM4174168	Control	nuclearRNA	r2
GSM4174169	KD	nuclearRNA	r1
GSM4174170	KD	nuclearRNA	r2

KD: Knock down.

Table 2. Sample tables for mESC.

GEO ID	Treatments	Observed	Replicates
GSM3912479	Control	H3K27ac	r1
GSM3912480	Control	H3K27ac	r2
GSM3912481	Control	H3K4me3	r1
GSM3912482	Control	H3K4me3	r2
GSM3912485	KO1	H3K27ac	r1
GSM3912486	KO1	H3K27ac	r2
GSM3912487	KO1	H3K4me3	r1
GSM3912488	KO1	H3K4me3	r2
GSM3912491	KO2	H3K27ac	r1
GSM3912492	KO2	H3K27ac	r2
GSM3912493	KO2	H3K4me3	r1
GSM3912494	KO2	H3K4me3	r2
GSM3912555	Control	nuclearRNA	r1
GSM3912556	Control	nuclearRNA	r2
GSM3912557	KO1	nuclearRNA	r1
GSM3912558	KO1	nuclearRNA	r2
GSM3912559	KO2	nuclearRNA	r1
GSM3912560	KO2	nuclearRNA	r2
GSM3912800	Control	MeRIP	r1
GSM3912801	Control	MeRIP	r2
GSM3912802	KO1	MeRIP	r1
GSM3912803	KO1	MeRIP	r2
GSM3912804	KO2	MeRIP	r1
GSM3912805	KO2	MeRIP	r2

KO: knock out.

2.2. Tensor

HEC-1-A and mESC datasets were formatted as tensors, $x_{ijks} \in \mathbb{R}^{N\times 4\times K\times 2}$, which represent jth measurements ($j = 1$: H3K4me3, $j = 2$: H3K27ac, $j = 3$: MeRIP, and $j = 4$: nascent nuclear RNA expression) of ith gene (Ensembl gene ID) of sth biological replicate of kth sample (for HEC-1-A, $K = 2$, $k = 1$: control and $k = 2$:KO; for mESC, $K = 3$, $k = 1$: control, $k = 2$: the 1st KO, and $k = 3$: the 2nd KO). Since the provided histone modifications as well as m6A were not mapped to individual genes to which Ensembl gene IDs are attributed, we had to integrate these values over each gene. To accomplish this, values assigned to the regions included fully within gene regions were integrated and assigned to individual genes (Ensembl gene ID). Finally, x_{ijks} were normalized as $\sum_i x_{ijks} = 0$ and $\sum_i x_{ijks}^2 = N$.

2.3. Tensor Decomposition-Based Unsupervised Feature Extraction

Higher order singular value decomposition [18] (HOSVD) was applied to x_{ijks} to derive tensor decomposition

$$x_{ijks} = \sum_{\ell_1=1}^{4}\sum_{\ell_2=1}^{K}\sum_{\ell_3=1}^{2}\sum_{\ell_4=1}^{N} G(\ell_1\ell_2\ell_3\ell_4)u_{\ell_1 j}u_{\ell_2 k}u_{\ell_3 s}u_{\ell_4 i} \quad (1)$$

where $G \in \mathbb{R}^{4\times K\times 2\times N}$ is a core tensor and $u_{\ell_1 j} \in \mathbb{R}^{4\times 4}, u_{\ell_2 k} \in \mathbb{R}^{K\times K}, u_{\ell_3 s} \in \mathbb{R}^{2\times 2}, u_{\ell_4 i} \in \mathbb{R}^{N\times N}$ are singular value matrices that are orthogonal matrices.

To select genes that are valid biologically, $u_{\ell_4 i}$ used for gene identification had to be specified. Therefore, we needed to find which of $u_{\ell_1 j}, u_{\ell_2 k}, u_{\ell_3 s}$ was biologically valid. Given ℓ_1, ℓ_2, ℓ_3, we sought $G(\ell_1\ell_2\ell_3\ell_4)$ that had larger absolute values, resulting in the selection of ℓ_4. After identifying $u_{\ell_4 i}$, we could address p-values to genes assuming that $u_{\ell_4 i}$ obeys a Gaussian distribution as

$$P_i = P_{\chi^2}\left[> \left(\frac{u_{\ell_4 i}}{\sigma_4}\right)^2\right] \quad (2)$$

where $P_{\chi^2}[> x]$ is a cumulative χ^2 distribution whose argument is larger than x and σ_4 is standard deviation. p-values were corrected by BH criterion [18] and genes (Ensemble gene IDs) associated with adjusted p-values less than 0.01 were selected.

2.4. Enrichment Analysis

Gene symbols associated and selected with Ensembl gene ID were retrieved by ID conversion tool implemented in DAVID [20] and were uploaded to Enrichr [21] in order to validate their biological features; TFs, pathways, and diseases associated with adjusted p-values less than 0.05 were identified as significant.

3. Results

3.1. Gene Selections

HOSVD was applied to tensors x_{ijks} of HEC-1-A and mESC (Figures 2 and 3). Independent of target species,

- u_{1j}, which is attributed to measurements, represents constant values for histone modifications, m6A, and nascent RNA; it likely exhibits transcription activated by m6A through histone modification.
- u_{2k} (and u_{3k} for mESC), which are both attributed to the distinction between METTL3 KO and control, exhibit the distinction between them; they are more likely related to mA6 mediated effects.
- u_{1s}, which is attributed to two biological replicates, represents constant values between two replicates; it likely exhibits features independent of replicates.

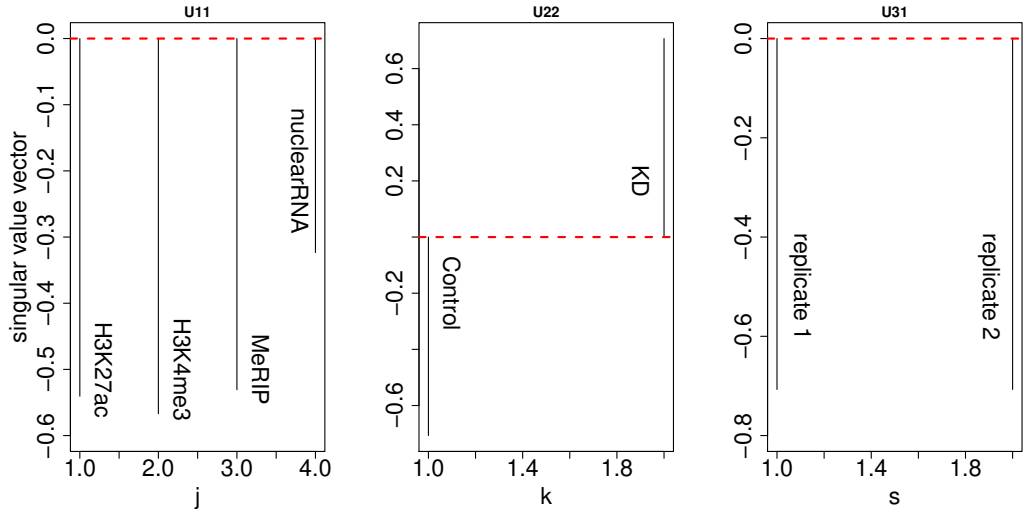

Figure 2. Singular value vectors obtained by applying HOSVD to HEC-1-A, x_{ijks}. U11: u_{1j}, U22: u_{2k}, U31: u_{1s}.

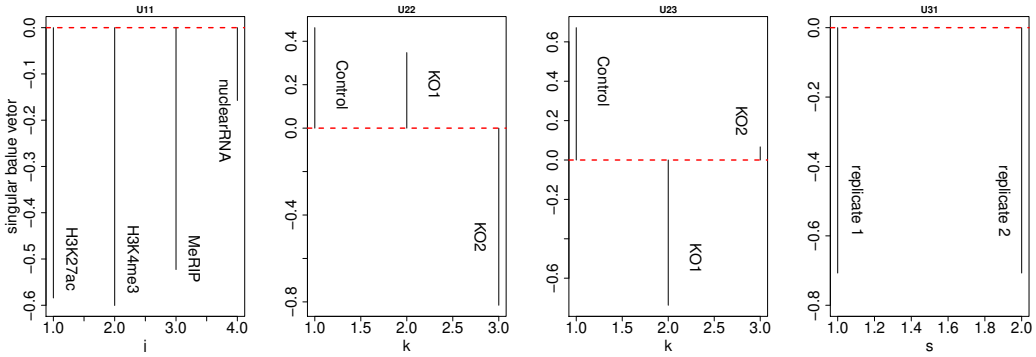

Figure 3. Singular value vectors obtained by applying HOSVD to mESC, x_{ijks}. U11: u_{1j}, U22: u_{2k}, U23: u_{3k}, U31: u_{1s}.

In general, singular value vectors exhibit the patterns of representative genes. The fact that u_{1j}s take constant values means that the amounts of histone modification, m6A, and nascent RNA simultaneously vary over some sets of genes, because otherwise such a singular value vector cannot appear. The fact that u_{3k}s take opposite signs between $k = 1$ and $k = 2$ means that there are some sets of genes whose amounts of histone modification, m6A, and nascent RNA are distinct between control and METTL3 KO, because otherwise such a singular value vector cannot appear. The fact that u_{1s}s take constant values means that the amounts of histone modification, m6A, and nascent RNA will be independent of biological replicates, because otherwise such a singular value vector cannot appear.

Next, we needed to identify which Gs had larger absolute values, given $\ell_1 = 1, \ell_2 = 2$ (and also 3 for mouse), and $\ell_3 = 1$. G represents the weight by which the combination of $u_{\ell_1 j} u_{\ell_2 k} u_{\ell_3 s} u_{\ell_4 i}$ contributes to x_{ijks} (Equation (1)), because $u_{\ell_1 j}, u_{\ell_2 k}, u_{\ell_3 s}$, and $u_{\ell_4 i}$ are unit vectors. Since we have already identified which $u_{\ell_1 j}, u_{\ell_2 k}$, and $u_{\ell_3 s}$ are associated with the properties of interest, by identifying which $G(\ell_1 \ell_2 \ell_3 \ell_4)$ has the largest absolute value given ℓ_1, ℓ_2, and ℓ_3, we can know which $u_{\ell_4 i}$ is most associated with the properties of interest.

Independent of target species, U_{5i} has the absolutely largest $G(1, 2, 1, \ell_4)$ (Table 3). Although one might wonder why $\ell_4 = 7$ was not employed in spite of that $|G(1, 3, 1, 7)| > |G(1, 3, 1, 5)|$, $\ell_4 = 5$ was selected because of larger $\sum_{\ell_2=2}^{3} G(1, \ell_2, 1, \ell_4)^2$. Following this, p-values were attributed to ith gene (Ensembl gene ID) using Equation (2). After correcting P_i using BH criterion [18], 740 human and 667 mouse genes with Ensembl gene ID were selected, respectively (full list is available as Supplementary Materials). After converting

Ensembl gene IDs into gene symbols using gene ID conversion tools implemented in DAVID [20], we investigated the intersection between these two sets of genes.

Table 3. $G(1,2,1,\ell_4)$ for human and mouse and $G(1,3,1,\ell_4)$ only for mice obtained by applying HOSVD to x_{ijks} of HAC-1-A (human) and mESC (mouse). Bold faced values were employed.

ℓ_4	Human	Mouse	
	$G(1,2,1,\ell_4)$		$G(1,3,1,\ell_4)$
1	−3.8580489	11.451996	0.3547811
2	−8.3420060	−3.105822	0.5361026
3	1.2758702	−1.979357	−15.3679662
4	0.4298687	21.579441	2.8415422
5	**−72.7824354**	**−82.092367**	**−31.1421313**
6	10.1455134	1.676667	19.6058307
7	−10.1008315	−7.248264	66.0183422
8	−10.3176091	5.825304	4.3903138
9	−1.4442934	38.314394	−23.3314778
10	0.3916004	6.841401	7.6772055

Figure 4 shows the Venn diagram between gene symbols selected using TD-based unsupervised FE. Fisher's exact test shows that the overlap is highly significant (Table 4).

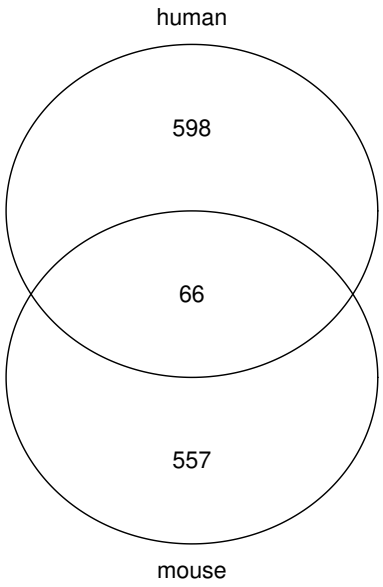

Figure 4. Venn diagram of gene symbols selected using TD-based unsupervised FE for mice (mESC) and humans (HEC-1-A).

Table 4. Confusion matrix of gene symbols selected by TD-based unsupervised FE between HAC-1-A (human) and mESC (mouse). Odds ratio is 4.00, $P = 1.91 \times 10^{-17}$. Since only common gene symbols between mice and humans were considered to generate the confusion matrix, the total number of genes considered was less than the total numbers of mouse and human genes respectively.

		Human	
		Not Selected	**Selected**
mouse	not selected	15704	496
	selected	499	63

This can be additional evidence that TD-based unsupervised FE is successful, since accidental significant overlaps between genes selected using two completely independent datasets are unlikely, although there is still some possibility that the coincidence between the two are not biological.

3.2. Transcription Factors Likely to Be Recruited by m6A

In order to identify transcription factors (TFs) that are likely recruited by m6A, we referred to "ENCODE and ChEA Consensus TFs from ChIP-X" category in Enrichr (full list is available as Supplementary Materials). This category is the consensus list between two independent research projects, ENCODE [22] and ChEA [23], where TF binding to human genome was comprehensively investigated by ChIP-Seq experiments.

There were 27 TFs commonly selected (Figure 5 and Table 5), which also suggests the success of TD-based unsupervised FE, since it is unlikely that there are significant overlaps between TFs selected using two independent datasets. Some of these TFs are reported to be related to open chromatin. AR [24] is related to chromatin accessibility. E2F1 is also reported to be associated with regulating chromatin components [25]. ESR1 [26] mediates allele-specific chromatin recruitment. GATA2 [27] mediates looped chromatin organization. KLF4 is involved in the organization and regulation of enhancer networks [28]. MYC drives chromatin accessibility [29]. NANOG establishes chromatin accessibility [30]. PPARγ binding induces open chromatin and histone acetylation (Figure 7 [31]). The interactomes of POU5F1 and SOX2 enhancers in human embryonic stem cells is observed [32]. SALL4 promotes glycolysis and chromatin remodeling [33]. STAT3 plays some roles in regulator of chromatin topology [34]. TP53 engages distinct local chromatin environments [35]. TP63 cooperates with CTCF to modulate chromatin architecture [36]. CHD1 regulates open chromatin [37]. RCOR1 is known as a chromatin regulator [38]. TAF1 has some relationship with histone acetyltransferases [39]. UBTF1 and UBTF2 bind to open chromatin structures [40]. YY1 was listed as one that promotes open chromatin and activates transcription [13]. ZBTB7A is a transducer for the control of promoter accessibility [41]. This also suggests that TD-based unsupervised FE identifies the potential TFs that regulate chromatin structure as expected.

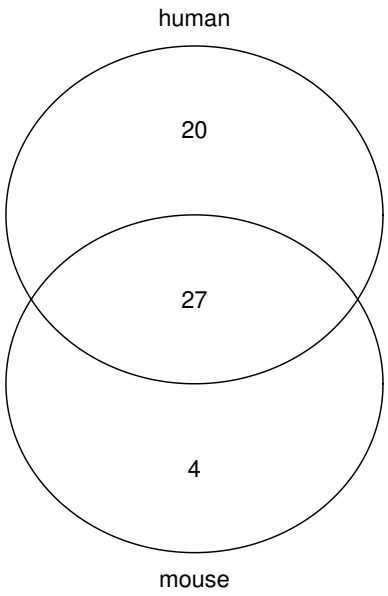

Figure 5. Venn diagram of TFs in "ENCODE and ChEA Consensus TFs from ChIP-X" category, selected by uploading genes selected by TD-based unsupervised FE to Enrichr.

Table 5. Twenty seven commonly selected TFs from Figure 5.

CHEA	AR E2F1 ESR1 GATA2 KLF4 MYC NANOG NFE2L2 PPARG POU5F1 SMAD4 SALL4 SOX2 STAT3 TP53 TP63
ENCODE	CHD1 CTCF PBX3 RCOR1 RELA TAF1 TCF3 UBTF YY1 ZBTB7A ZNF384

In addition to such literature as mentioned above, we also tried to identify interactions between TFs and enrichment analysis of TFs themselves.

Not only are they tightly interrelated, but also the four representative TFs, MYC, STAT3, SMAD4, and TP53, regulate most of these TFs. This strongly suggests that TD-based unsupervised FE successfully identified genes that are important parts of the regulatory network.

It is also interesting to see what kind of biological processes are controlled by the TF network shown in Figure 6. In order to see this, we uploaded 27 TFs to REACTOME [42] (Table 6).

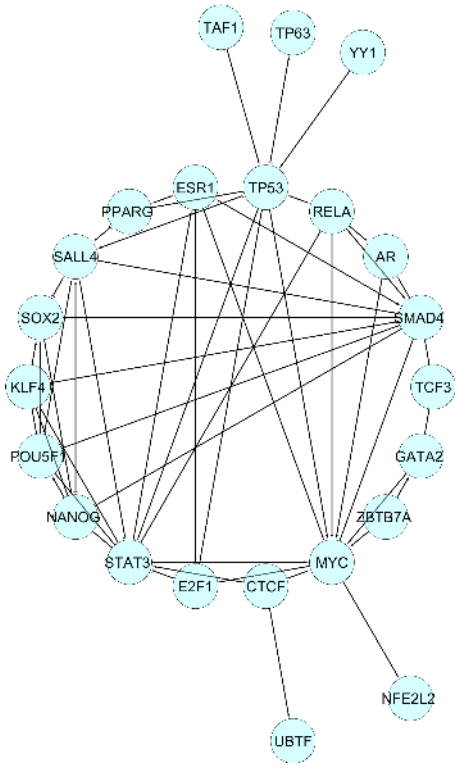

Figure 6. The networks between 27 TFs are listed in Table 5 retrieved from TRRUST2 [43]. Full information is available as Supplementary Material.

First of all, there are many transcription regulation-related pathways that are enriched in candidate TFs that m6A recruits. Second, there are many descriptions that suggest the relationship with chromatin reorganizations (see Supplementary Materials). For example, TFs that belong to "Generic Transcription Pathway" are known to act as co-activator and co-repressor complexes that affect histone modifications. TFs that belong to "Gene expression" are known to cause epigenetic changes that result in altered chromatin complexes that influence transcription. TFs that belong to "Estrogen-dependent gene expression" are known to establish active chromatin marks. Thus, from the points of functions also, these TFs are very suitable to be recruited by m6A.

Table 6. REACTOME enrichment analysis for 27 TFs in Table 5.

Pathway Name	Found	Ratio	*p*-Value	FDR
Transcriptional regulation of pluripotent stem cells	13/45	3.00×10^{-3}	1.11×10^{-16}	3.76×10^{-14}
Developmental Biology	23/1241	8.50×10^{-2}	2.35×10^{-12}	3.97×10^{-10}
Generic Transcription Pathway	24/1554	1.06×10^{-1}	2.99×10^{-11}	3.38×10^{-9}
POU5F1 (OCT4), SOX2, NANOG activate genes related to proliferation	6/21	1.00×10^{-3}	1.29×10^{-10}	1.01×10^{-8}
Gene expression (Transcription)	25/1851	1.26×10^{-1}	1.67×10^{-10}	1.01×10^{-8}
RNA Polymerase II Transcription	24/1693	1.15×10^{-1}	1.80×10^{-10}	1.01×10^{-8}
Interleukin-4 and Interleukin-13 signaling	9/211	1.40×10^{-2}	3.87×10^{-8}	1.86×10^{-6}
ESR-mediated signaling	9/256	1.70×10^{-2}	1.97×10^{-7}	8.26×10^{-6}
Estrogen-dependent gene expression	7/154	1.00×10^{-2}	9.44×10^{-7}	3.49×10^{-5}
Transcriptional regulation of granulopoiesis	5/71	5.00×10^{-3}	4.69×10^{-6}	1.33×10^{-4}
Signaling by Nuclear Receptors	9/385	2.60×10^{-2}	5.57×10^{-6}	1.33×10^{-4}
POU5F1 (OCT4), SOX2, NANOG repress genes related to differentiation	3/10	6.82×10^{-4}	6.06×10^{-6}	1.33×10^{-4}
Binding of TCF/LEF:CTNNB1 to target gene promoters	3/10	6.82×10^{-4}	6.06×10^{-6}	1.33×10^{-4}
Activation of PUMA and translocation to mitochondria	3/10	6.82×10^{-4}	6.06×10^{-6}	1.33×10^{-4}
RUNX3 regulates WNT signaling	3/10	6.82×10^{-4}	6.06×10^{-6}	1.33×10^{-4}
Repression of WNT target genes	3/16	1.00×10^{-3}	2.45×10^{-5}	5.14×10^{-4}
Transcriptional regulation by the AP-2 (TFAP2) family of transcription factors	4/52	4.00×10^{-3}	3.19×10^{-5}	6.06×10^{-4}
TP53 Regulates Transcription of Genes Involved in G1 Cell Cycle Arrest	3/20	1.00×10^{-3}	4.73×10^{-5}	8.44×10^{-4}
Signaling by Interleukins	10/639	4.40×10^{-2}	5.07×10^{-5}	8.44×10^{-4}
Transcriptional regulation by RUNX3	5/118	8.00×10^{-3}	5.27×10^{-5}	8.44×10^{-4}
TFAP2 (AP-2) family regulates transcription of growth factors and their receptors	3/21	1.00×10^{-3}	5.46×10^{-5}	8.74×10^{-4}
Intrinsic Pathway for Apoptosis	4/61	4.00×10^{-3}	5.90×10^{-5}	8.86×10^{-4}

3.3. Biological Processes

Genes identified by TD-based unsupervised FE seem to successfully identify TFs recruited by m6A. It is more interesting to know the kind of biological processes that are mediated by those identified genes. For that, we investigated the "KEGG 2019 Human" category in Enrichr (full list is available in Supplementary Materials). This category is a list of genes included in the pathways that Kyoto Encyclopedia of Genes and Genomes (KEGG) [44] provided. KEGG is a collection of pathways that are experimentally validated. Based upon the biological considerations, various pathways are identified, along with genes and compounds that take part in individual pathways.

There are six KEGG pathways commonly selected (Figure 7 and Table 7), which also suggest the success of TD-based unsupervised FE, since it is unlikely that there are significant overlaps between pathways selected using two independent datasets.

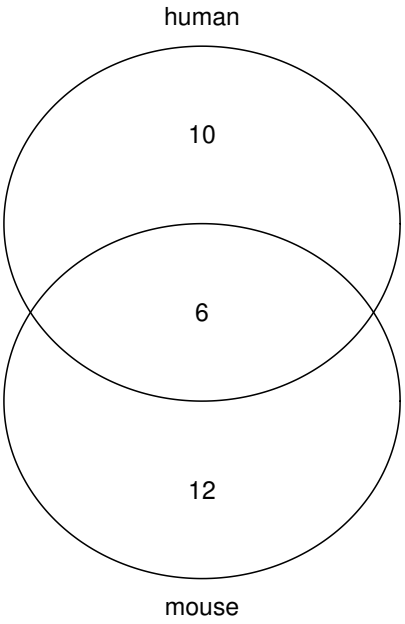

Figure 7. Venn diagram of KEGG pathways in "KEGG 2019 Human" category, selected by uploading genes selected by TD-based unsupervised FE to Enrichr.

Table 7. Six commonly selected KEGG pathways from Figure 7.

"Regulation of actin cytoskeleton"; "Adherens junction"; "Focal adhesion"; "Rap1 signaling pathway"; "Ras signaling pathway"; "Proteoglycans in cancer"

There are many known studies that relate these pathways to m6A. A handful of genes were associated with the formation of the adherens junction and the actin cytoskeleton in cancer cells were undergoing epithelial-mesenchymal transition [45]. According to the number of open reading frames and m6A, Chen et al. identified 224 circRNAs with coding potential, and performed GO and KEGG analyses based on the linear counterparts of 75 circRNAs. They determined that the 75 circRNAs were related to regulating the actin cytoskeleton and metabolic pathways [46]. Ras signaling pathway [47] and Rap1 signaling pathway [48] are related to actin cytoskeleton. Thus, TD-based unsupervised FE identified genes enriched in KEGG pathways known to be related to m6A.

We also investigated "Reactome 2016." Reactome [42] is yet another pathways database. Although it is very similar to KEGG, it has its own definitions of paythways.

There were six Reactome pathways commonly selected (Figure 8 and Table 8), which also suggested the success of TD-based unsupervised FE, since the possibility of significant overlaps between pathways selected using two independent datasets is highly unlikely. m6A was widely investigated to consider relationship with brain function [49–52]; these pathways are generally known to be related to brain functions. The relationship between axon guidance and brain function is obvious. Developmental biology is related to this pathway as well, while SMADs is related to cell development [53]. Rho GTPases play some roles in neuronal morphogenesis [54]. Nephrin is expressed in adult rodent central nervous system [55]. The L1CAM family has been implicated in processes integral to nervous system development (R-HSA-373760). Thus, the detection of these pathways might help us understand the function of m6A in brain functions.

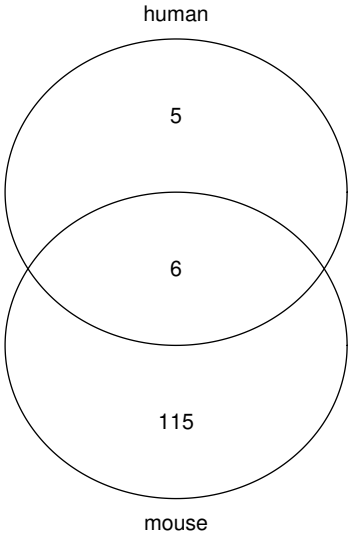

Figure 8. Venn diagram of REACTOME pathways in "Reactome 2016" category, selected by uploading genes selected by TD-based unsupervised FE to Enrichr.

Table 8. Six commonly selected KEGG pathways from Figure 8.

"Developmental Biology Homo sapiens R-HSA-1266738"; "Axon guidance Homo sapiens R-HSA-422475"; "Downregulation of SMAD2/3:SMAD4 transcriptional activity Homo sapiens R-HSA-2173795"; "L1CAM interactions Homo sapiens R-HSA-373760"; "Nephrin interactions Homo sapiens R-HSA-373753"; "Signaling by Rho GTPases Homo sapiens R-HSA-194315"

In order to confirm whether genes selected by TD-based unsupervised FE are related to the brain, we investigated "ARCHS4 Tissues". ARCHS4 is a massive mine of publicly available RNA-seq data from humans and mice [56]. This category detects enhancements of tissue-related genes from ARCHS4.

There were four tissues commonly selected (Figure 9 and Table 9). Two out of four tissues, NEURONAL EPITHELIUM and ASTROCYTE were related to brains. Thus, TD-based unsupervised FE could identify brain functions mediated by m6A.

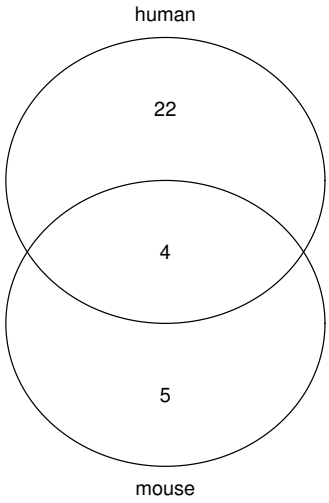

Figure 9. Venn diagram of tissues in "ARCHS4 Tissues" category, selected by uploading genes selected by TD-based unsupervised FE to Enrichr.

Table 9. Four commonly selected tissues from Figure 9.

"NEURONAL EPITHELIUM"; "PLACENTA (BULK)"; "ASTROCYTE"; "FIBROBLAST"

3.4. Diseases Mediated by m6A

It would be interesting for us to see whether some diseases are mediated by m6A. Therefore, we investigated "Disease Perturbations from GEO down" and "Disease Perturbations from GEO up". This category comprehensively collected up/down regulated genes in individual experiments included in GEO [19].

There were ten and four diseases commonly selected (Figure 10 and Table 10), which also suggests the success of TD-based unsupervised FE, since it is unlikely that there could be significant overlaps between diseases selected using two independent datasets. There were some studies that were coincident with these diseases; m6A was reported to be related to inflammatory bowel disease, which is a common chronic inflammatory gastrointestinal disorder whose major subtypes are Crohn's disease and ulcerative colitis [57]. m6A mediates pancreatic cancer [58,59]. m6A modifications of hepatitis B and C viral RNAs were reported to attenuate innate host immunity via RIG-I signaling [60]. Comprehensive analysis of m6A regulators was shown to possess prognostic value in prostate cancer [61]. m6A regulators were shown to contribute to malignant progression and survival prediction in chronic lymphocytic leukemia [62]. Thus, TD-based unsupervised FE successfully identified the diseases related to m6A.

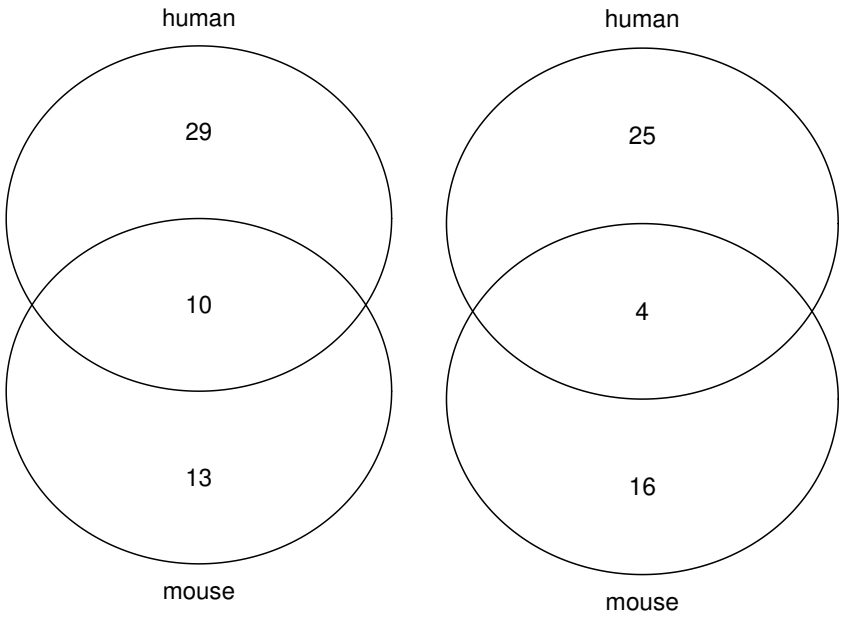

Figure 10. Venn diagram of diseases in "Disease Perturbations from GEO down" (**left**) and "Disease Perturbations from GEO up" (**right**) categories, selected by uploading genes selected by TD-based unsupervised FE to Enrichr.

Table 10. Ten and four commonly selected diseases from Figure 10.

Disease Perturbations from GEO down
"Crohn's disease DOID-8778 human GSE6731 sample 757"; "Ulcerative Colitis C0009324 human GSE6731 sample 249"; "Ulcerative colitis DOID-8577 human GSE6731 sample 759"; "Ulcerative colitis DOID-8577 human GSE6731 sample 760"; "Hepatitis C DOID-1883 human GSE20948 sample 599"; "Diabetic Nephropathy C0011881 human GSE1009 sample 223"; "Cardiac Hypertrophy C1383860 rat GSE1055 sample 354"; "Prostate cancer DOID-10283 human GSE3868 sample 639"; "Hepatitis C DOID-1883 human GSE20948 sample 597"; "Cancer of prostate C0376358 human GSE3868 sample 135"
Disease Perturbations from GEO up
"Pancreatitis DOID-4989 mouse GSE3644 sample 513 Asthma"; "Allergic C0155877 human GSE3004 sample 360"; "Acute pancreatitis C0001339 mouse GSE3644 sample 376"; "Chronic lymphocytic leukemia DOID-1040 human GSE6691 sample 786"

4. Discussion

First of all, we identified genes, TFs, pathways, and diseases common between analyses using the mouse and human samples. Since they are independent datasets, it is very unlikely that these coincidences were accidental. Although genes commonly selected between human and mouse are as little as ten percent (Figure 4), identified TFs, pathways, and diseases were largely overlapped for humans and mice (Figures 5, 7, 8, and 10). Since so many overlaps cannot be obtained accidentally, these results strongly support the reliability of our findings.

In addition to this, the identified genes, TFs, pathways, and diseases are largely associated with previous studies that support these findings. TFs were reported to contribute to chromatin structures, pathways identified were previously reported to be related to m6A, and some studies have reported the relationships between diseases and m6A. This suggests that TD-based unsupervised FE has a superior ability to identify biologically valid relationships to m6A, using very small sized datasets composed of only two biological replicates. The results derived here might help us understand how m6A regulates transcriptions.

One might wonder why only 27 TFs are detected, and about other TFs. It is obvious that m6A does regulate transcription not only through TFs but also through many other factors which have not yet been known. At the moment, we do not know how to figure out other factors through which m6A regulates transcription. It will be an important issue to be addressed in the future.

5. Conclusions

In this paper, using TD-based unsupervised FE, we successfully identified key genes that could allow us to identify key TFs, pathways, and diseases mediated by m6A.

Supplementary Materials: The following are available online at https://www.mdpi.com/2076-3417/11/1/213/s1, full list of selected genes, full list of enrichment analyses by Enrichr, enrichment analysis by REACTOME, and details of the results by TRRUST2.

Author Contributions: Conceptualization, Y.-h.T. and M.M.G.; methodology, Y.-h.T.; software, Y.-h.T.; validation, Y.-h.T., M.M.G., and S.A.P.D.; formal analysis, Y.-h.T.; investigation, Y.-h.T.; writing—original draft preparation, Y.-h.T.; writing—review and editing, Y.-h.T., M.M.G., and S.A.P.D.; visualization, Y.-h.T.; supervision, Y.-h.T.; project administration, Y.-h.T.; funding acquisition, Y.-h.T. All authors have read and agreed to the published version of the manuscript.

Funding: This research was funded by the Grants-in-Aid for Scientific Research (KAKENHI), 20H04848, 20K12067, 19H05270.

Institutional Review Board Statement: Not applicable.

Informed Consent Statement: Not applicable.

Data Availability Statement: All data used in this study is publically available in GEO as stated in Materials and Methods.

Conflicts of Interest: The authors declare no conflict of interest. The funders had no role (1) in the design of the study, (2) in the collection, analyses, or interpretation of data, (3) in the writing of the manuscript, or (4) in the decision to publish the results.

Abbreviations

The following abbreviations are used in this manuscript:

TD	tensor decomposition
TF	transcription factor
FE	feature extraction
HOSVD	higher order singular value decomposition
mESC	mouse embryonic stem cell

References

1. Martin, J. Epitranscriptomics: Mapping methods and beyond. *BioTechniques* **2018**, *65*, 121–124. [CrossRef] [PubMed]
2. Nishikura, K. A-to-I editing of coding and non-coding RNAs by ADARs. *Nat. Rev. Mol. Cell Biol.* **2015**, *17*, 83–96. [CrossRef] [PubMed]
3. Vu, L.T.; Tsukahara, T. C-to-U editing and site-directed RNA editing for the correction of genetic mutations. *BioSci. Trends* **2017**, *11*, 243–253. [CrossRef] [PubMed]
4. Bokar, J.A.; Shambaugh, M.E.; Polayes, D.; Matera, A.G.; Rottman, F.M. Purification and cDNA cloning of the AdoMet-binding subunit of the human mRNA (N6-adenosine)-methyltransferase. *RNA* **1997**, *3*, 1233–1247. Available online: https://rnajournal.cshlp.org/content/3/11/1233 (accessed on 27 December 2020).
5. Liu, J.; Yue, Y.; Han, D.; Wang, X.; Fu, Y.; Zhang, L.; Jia, G.; Yu, M.; Lu, Z.; Deng, X.; et al. A METTL3–METTL14 complex mediates mammalian nuclear RNA N6-adenosine methylation. *Nat. Chem. Biol.* **2013**, *10*, 93–95. [CrossRef] [PubMed]
6. Fazi, F.; Fatica, A. Interplay Between N6-Methyladenosine (m6A) and Non-coding RNAs in Cell Development and Cancer. *Front. Cell Dev. Biol.* **2019**, *7*, 116. [CrossRef]
7. An, S.; Zhang, J.; Wang, Y.; Zhang, Y.; Liu, Q. The Roles of N6-Methyladenosine in Human Diseases. *Biochem. Insights* **2019**, *12*. [CrossRef]
8. Huang, H.; Camats-Perna, J.; Medeiros, R.; Anggono, V.; Widagdo, J. Altered Expression of the m6A Methyltransferase METTL3 in Alzheimer's Disease. *Eneuro* **2020**. [CrossRef]
9. Qin, L.; Min, S.; Shu, L.; Pan, H.; Zhong, J.; Guo, J.; Sun, Q.; Yan, X.; Chen, C.; Tang, B.; et al. Genetic analysis of N6-methyladenosine modification genes in Parkinson's disease. *Neurobiol. Aging* **2020**, *93*, 143.e9–143.e13. [CrossRef]
10. He, L.; Li, H.; Wu, A.; Peng, Y.; Shu, G.; Yin, G. Functions of N6-methyladenosine and its role in cancer. *Mol. Cancer* **2019**, *18*. [CrossRef]
11. Winkler, R.; Gillis, E.; Lasman, L.; Safra, M.; Geula, S.; Soyris, C.; Nachshon, A.; Tai-Schmiedel, J.; Friedman, N.; Le-Trilling, V.T.K.; et al. m6A modification controls the innate immune response to infection by targeting type I interferons. *Nat. Immunol.* **2018**, *20*, 173–182. [CrossRef]
12. Huang, H.; Weng, H.; Zhou, K.; Wu, T.; Zhao, B.S.; Sun, M.; Chen, Z.; Deng, X.; Xiao, G.; Auer, F.; et al. Histone H3 trimethylation at lysine 36 guides m6A RNA modification co-transcriptionally. *Nature* **2019**, *567*, 414–419. [CrossRef] [PubMed]
13. Liu, J.; Dou, X.; Chen, C.; Chen, C.; Liu, C.; Xu, M.M.; Zhao, S.; Shen, B.; Gao, Y.; Han, D.; et al. N6-methyladenosine of chromosome-associated regulatory RNA regulates chromatin state and transcription. *Science* **2020**, *367*, 580–586. [CrossRef] [PubMed]
14. Chen, Y.G.; Chen, R.; Ahmad, S.; Verma, R.; Kasturi, S.P.; Amaya, L.; Broughton, J.P.; Kim, J.; Cadena, C.; Pulendran, B.; et al. N6-Methyladenosine Modification Controls Circular RNA Immunity. *Mol. Cell* **2019**, *76*, 96–109.e9. [CrossRef] [PubMed]
15. Akhtar, J.; Renaud, Y.; Albrecht, S.; Ghavi-Helm, Y.; Roignant, J.Y.; Silies, M.; Junion, G. m6A RNA methylation regulates promoter proximal pausing of RNA Polymerase II. *bioRxiv* **2020**. [CrossRef]
16. Zhou, K.I.; Shi, H.; Lyu, R.; Wylder, A.C.; Matuszek, Ż.; Pan, J.N.; He, C.; Parisien, M.; Pan, T. Regulation of Co-transcriptional Pre-mRNA Splicing by m6A through the Low-Complexity Protein hnRNPG. *Mol. Cell* **2019**, *76*, 70–81.e9. [CrossRef]
17. Yang, X.; Liu, Q.L.; Xu, W.; Zhang, Y.C.; Yang, Y.; Ju, L.F.; Chen, J.; Chen, Y.S.; Li, K.; Ren, J.; et al. m6A promotes R-loop formation to facilitate transcription termination. *Cell Res.* **2019**, *29*, 1035–1038. [CrossRef]
18. Taguchi, Y.H. *Unsupervised Feature Extraction Applied to Bioinformatics*; Springer International Publishing: Berlin/Heidelberg, Germany, 2020, doi:10.1007/978-3-030-22456-1. [CrossRef]
19. Barrett, T.; Wilhite, S.E.; Ledoux, P.; Evangelista, C.; Kim, I.F.; Tomashevsky, M.; Marshall, K.A.; Phillippy, K.H.; Sherman, P.M.; Holko, M.; et al. NCBI GEO: Archive for functional genomics data sets-update. *Nucleic Acids Res.* **2012**, *41*, D991–D995. [CrossRef]

20. Huang, D.W.; Sherman, B.T.; Lempicki, R.A. Systematic and integrative analysis of large gene lists using DAVID bioinformatics resources. *Nat. Protoc.* **2008**, *4*, 44–57. [CrossRef]
21. Kuleshov, M.V.; Jones, M.R.; Rouillard, A.D.; Fernandez, N.F.; Duan, Q.; Wang, Z.; Koplev, S.; Jenkins, S.L.; Jagodnik, K.M.; Lachmann, A.; et al. Enrichr: A comprehensive gene set enrichment analysis web server 2016 update. *Nucleic Acids Res.* **2016**, *44*, W90–W97. [CrossRef]
22. An integrated encyclopedia of DNA elements in the human genome. *Nature* **2012**, *489*, 57–74. [CrossRef]
23. Lachmann, A.; Xu, H.; Krishnan, J.; Berger, S.I.; Mazloom, A.R.; Ma'ayan, A. ChEA: Transcription factor regulation inferred from integrating genome-wide ChIP-X experiments. *Bioinformatics* **2010**, *26*, 2438–2444. [CrossRef] [PubMed]
24. Tewari, A.K.; Yardimci, G.; Shibata, Y.; Sheffield, N.C.; Song, L.; Taylor, B.S.; Georgiev, S.G.; Coetzee, G.A.; Ohler, U.; Furey, T.S.; et al. Chromatin accessibility reveals insights into androgen receptor activation and transcriptional specificity. *Genome Biol.* **2012**, *13*, R88. [CrossRef] [PubMed]
25. Magri, L.; Swiss, V.A.; Jablonska, B.; Lei, L.; Pedre, X.; Walsh, M.; Zhang, W.; Gallo, V.; Canoll, P.; Casaccia, P. E2F1 Coregulates Cell Cycle Genes and Chromatin Components during the Transition of Oligodendrocyte Progenitors from Proliferation to Differentiation. *J. Neurosci.* **2014**, *34*, 1481–1493. [CrossRef] [PubMed]
26. Jeselsohn, R.; Bergholz, J.S.; Pun, M.; Cornwell, M.; Liu, W.; Nardone, A.; Xiao, T.; Li, W.; Qiu, X.; Buchwalter, G.; et al. Allele-Specific Chromatin Recruitment and Therapeutic Vulnerabilities of ESR1 Activating Mutations. *Cancer Cell* **2018**, *33*, 173–186.e5. [CrossRef] [PubMed]
27. Jing, H.; Vakoc, C.R.; Ying, L.; Mandat, S.; Wang, H.; Zheng, X.; Blobel, G.A. Exchange of GATA Factors Mediates Transitions in Looped Chromatin Organization at a Developmentally Regulated Gene Locus. *Mol. Cell* **2008**, *29*, 232–242. [CrossRef] [PubMed]
28. Giammartino, D.C.D.; Kloetgen, A.; Polyzos, A.; Liu, Y.; Kim, D.; Murphy, D.; Abuhashem, A.; Cavaliere, P.; Aronson, B.; Shah, V.; et al. KLF4 is involved in the organization and regulation of pluripotency-associated three-dimensional enhancer networks. *Nat. Cell Biol.* **2019**, *21*, 1179–1190. [CrossRef] [PubMed]
29. Nepon-Sixt, B.S.; Bryant, V.L.; Alexandrow, M.G. Myc-driven chromatin accessibility regulates Cdc45 assembly into CMG helicases. *Commun. Biol.* **2019**, *2*. [CrossRef]
30. Pálfy, M.; Schulze, G.; Valen, E.; Vastenhouw, N.L. Chromatin accessibility established by Pou5f3, Sox19b and Nanog primes genes for activity during zebrafish genome activation. *PLoS Genet.* **2020**, *16*, 1–25. [CrossRef]
31. Lefterova, M.I.; Steger, D.J.; Zhuo, D.; Qatanani, M.; Mullican, S.E.; Tuteja, G.; Manduchi, E.; Grant, G.R.; Lazar, M.A. Cell-Specific Determinants of Peroxisome Proliferator-Activated Receptor Function in Adipocytes and Macrophages. *Mol. Cell. Biol.* **2010**, *30*, 2078–2089. [CrossRef]
32. Gao, F.; Wei, Z.; An, W.; Wang, K.; Lu, W. The interactomes of POU5F1 and SOX2 enhancers in human embryonic stem cells. *Sci. Rep.* **2013**, *3*. [CrossRef]
33. Kim, J.; Xu, S.; Xiong, L.; Yu, L.; Fu, X.; Xu, Y. SALL4 promotes glycolysis and chromatin remodeling via modulating HP1α-Glut1 pathway. *Oncogene* **2017**, *36*, 6472–6479. [CrossRef] [PubMed]
34. Zhao, Y.; Zeng, C.; Tarasova, N.I.; Chasovskikh, S.; Dritschilo, A.; Timofeeva, O.A. A new role for STAT3 as a regulator of chromatin topology. *Transcription* **2013**, *4*, 227–231. [CrossRef] [PubMed]
35. Sammons, M.A.; Zhu, J.; Drake, A.M.; Berger, S.L. TP53 engagement with the genome occurs in distinct local chromatin environments via pioneer factor activity. *Genome Res.* **2014**, *25*, 179–188. [CrossRef] [PubMed]
36. Qu, J.; Yi, G.; Zhou, H. p63 cooperates with CTCF to modulate chromatin architecture in skin keratinocytes. *Epigenet. Chromatin* **2019**, *12*. [CrossRef] [PubMed]
37. Gaspar-Maia, A.; Alajem, A.; Polesso, F.; Sridharan, R.; Mason, M.J.; Heidersbach, A.; Ramalho-Santos, J.; McManus, M.T.; Plath, K.; Meshorer, E.; et al. Chd1 regulates open chromatin and pluripotency of embryonic stem cells. *Nature* **2009**, *460*, 863–868. [CrossRef] [PubMed]
38. Boxer, L.D.; Barajas, B.; Tao, S.; Zhang, J.; Khavari, P.A. ZNF750 interacts with KLF4 and RCOR1, KDM1A, and CTBP1/2 chromatin regulators to repress epidermal progenitor genes and induce differentiation genes. *Genes Dev.* **2014**, *28*, 2013–2026. [CrossRef]
39. Durant, M.; Pugh, B.F. Genome-Wide Relationships between TAF1 and Histone Acetyltransferases in Saccharomyces cerevisiae. *Mol. Cell. Biol.* **2006**, *26*, 2791–2802. [CrossRef]
40. Sanij, E.; Diesch, J.; Lesmana, A.; Poortinga, G.; Hein, N.; Lidgerwood, G.; Cameron, D.P.; Ellul, J.; Goodall, G.J.; Wong, L.H.; et al. A novel role for the Pol I transcription factor UBTF in maintaining genome stability through the regulation of highly transcribed Pol II genes. *Genome Res.* **2015**, *25*, 201–212. [CrossRef]
41. Ramos Pittol, J.M.; Oruba, A.; Mittler, G.; Saccani, S.; van Essen, D. Zbtb7a is a transducer for the control of promoter accessibility by NF-kappa B and multiple other transcription factors. *PLoS Biol.* **2018**, *16*, 1–33. [CrossRef]
42. Jassal, B.; Matthews, L.; Viteri, G.; Gong, C.; Lorente, P.; Fabregat, A.; Sidiropoulos, K.; Cook, J.; Gillespie, M.; Haw, R.; et al. The reactome pathway knowledgebase. *Nucleic Acids Res.* **2019**, *48*, D498–D503. [CrossRef]
43. Han, H.; Cho, J.W.; Lee, S.; Yun, A.; Kim, H.; Bae, D.; Yang, S.; Kim, C.Y.; Lee, M.; Kim, E.; et al. TRRUST v2: An expanded reference database of human and mouse transcriptional regulatory interactions. *Nucleic Acids Res.* **2017**, *46*, D380–D386. [CrossRef] [PubMed]
44. Kanehisa, M.; Furumichi, M.; Sato, Y.; Ishiguro-Watanabe, M.; Tanabe, M. KEGG: Integrating viruses and cellular organisms. *Nucleic Acids Res.* **2020**, gkaa970. [CrossRef] [PubMed]

45. Lin, X.; Chai, G.; Wu, Y.; Li, J.; Chen, F.; Liu, J.; Luo, G.; Tauler, J.; Du, J.; Lin, S.; et al. RNA m6A methylation regulates the epithelial mesenchymal transition of cancer cells and translation of Snail. *Nat. Commun.* **2019**, *10*. [CrossRef] [PubMed]
46. Chen, R.; Jiang, T.; Lei, S.; She, Y.; Shi, H.; Zhou, S.; Ou, J.; Liu, Y. Expression of circular RNAs during C2C12 myoblast differentiation and prediction of coding potential based on the number of open reading frames and N6-methyladenosine motifs. *Cell Cycle* **2018**, *17*, 1832–1845. [CrossRef]
47. Prendergast, G.C.; Gibbs, J.B. *Pathways of Ras Function: Connections to the Actin Cytoskeleton*; Advances in Cancer Research; Academic Press: Cambridge, MA, USA, 1993; Volume 62, pp. 19–64. [CrossRef]
48. Wang, J.C.; Lee, J.Y.J.; Christian, S.; Dang-Lawson, M.; Pritchard, C.; Freeman, S.A.; Gold, M.R. The Rap1-cofilin pathway coordinates actin reorganization and MTOC polarization at the B-cell immune synapse. *J. Cell Sci.* **2017**, *130*, 1094–1109. [CrossRef] [PubMed]
49. Yu, J.; Zhang, Y.; Ma, H.; Zeng, R.; Liu, R.; Wang, P.; Jin, X.; Zhao, Y. Epitranscriptomic profiling of N6-methyladenosine-related RNA methylation in rat cerebral cortex following traumatic brain injury. *Mol. Brain* **2020**, *13*. [CrossRef]
50. Livneh, I.; Moshitch-Moshkovitz, S.; Amariglio, N.; Rechavi, G.; Dominissini, D. The m6A epitranscriptome: Transcriptome plasticity in brain development and function. *Nat. Rev. Neurosci.* **2019**, *21*, 36–51. [CrossRef]
51. Widagdo, J.; Anggono, V. The m6A-epitranscriptomic signature in neurobiology: From neurodevelopment to brain plasticity. *J. Neurochem.* **2018**, *147*, 137–152. [CrossRef]
52. Engel, M.; Eggert, C.; Kaplick, P.M.; Eder, M.; Röh, S.; Tietze, L.; Namendorf, C.; Arloth, J.; Weber, P.; Rex-Haffner, M.; et al. The Role of m6A/m-RNA Methylation in Stress Response Regulation. *Neuron* **2018**, *99*, 389–403.e9. [CrossRef]
53. Ueberham, U.; Arendt, T. The Role of Smad Proteins for Development, Differentiation and Dedifferentiation of Neurons. In *Trends in Cell Signaling Pathways in Neuronal Fate Decision*; InTech: London, UK, 2013. [CrossRef]
54. Luo, L. RHO GTPASES in neuronal morphogenesis. *Nat. Rev. Neurosci.* **2000**, *1*, 173–180. [CrossRef]
55. Li, M.; Armelloni, S.; Ikehata, M.; Corbelli, A.; Pesaresi, M.; Calvaresi, N.; Giardino, L.; Mattinzoli, D.; Nisticò, F.; Andreoni, S.; et al. Nephrin expression in the adult rodent central nervous system and its interaction with glutamate receptors. *J. Pathol.* **2011**, *225*, 118–128. [CrossRef] [PubMed]
56. Lachmann, A.; Torre, D.; Keenan, A.B.; Jagodnik, K.M.; Lee, H.J.; Wang, L.; Silverstein, M.C.; Ma'ayan, A. Massive mining of publicly available RNA-seq data from human and mouse. *Nat. Commun.* **2018**, *9*. [CrossRef] [PubMed]
57. Sebastian-delaCruz, M.; Olazagoitia-Garmendia, A.; Gonzalez-Moro, I.; Santin, I.; Garcia-Etxebarria, K.; Castellanos-Rubio, A. Implication of m6A mRNA Methylation in Susceptibility to Inflammatory Bowel Disease. *Epigenomes* **2020**, *4*, 16. [CrossRef]
58. Taketo, K.; Konno, M.; Asai, A.; Koseki, J.; Toratani, M.; Satoh, T.; Doki, Y.; Mori, M.; Ishii, H.; Ogawa, K. The epitranscriptome m6A writer METTL3 promotes chemo- and radioresistance in pancreatic cancer cells. *Int. J. Oncol.* **2017**. [CrossRef] [PubMed]
59. Geng, Y.; Guan, R.; Hong, W.; Huang, B.; Liu, P.; Guo, X.; Hu, S.; Yu, M.; Hou, B. Identification of m6A-related genes and m6A RNA methylation regulators in pancreatic cancer and their association with survival. *Ann. Transl. Med.* **2020**, *8*, 387. [CrossRef] [PubMed]
60. Kim, G.W.; Imam, H.; Khan, M.; Siddiqui, A. N6-Methyladenosine Modification of Hepatitis B and C Viral RNAs Attenuates Host Innate Immunity via RIG-I Signaling. *J. Biol. Chem.* **2020**. [CrossRef]
61. Ji, G.; Huang, C.; He, S.; Gong, Y.; Song, G.; Li, X.; Zhou, L. Comprehensive analysis of m6A regulators prognostic value in prostate cancer. *Aging* **2020**, *12*, 14863–14884. [CrossRef]
62. Zhang, Y.; Fang, X.; Chen, N.; Lv, X.; Ge, X.; Lu, K.; Zhou, X.; Yang, J.; Han, Y.; Hu, S.; et al. N6-Methyladenosine RNA Methylation Regulators Contribute to Malignant Progression and Survival Prediction in Chronic Lymphocytic Leukemia. *Blood* **2019**, *134*, 1738. [CrossRef]